Electron Transfer Dynamics and Surface Coverages of Binary Anthraquinone Monolayers on Mercury Microelectrodes

Robert J. Forster

School of Chemical Sciences, Dublin City University, Dublin 9, Ireland

Received November 7, 1994. In Final Form: February 28, 1995[⊗]

Single component monolayers of anthraquinone-2,6-disulfonic acid (2,6-AQDS) or anthraquinone-1,5-disulfonic acid (1,5-AQDS) have been formed by equilibrium adsorption from aqueous 1.0 M $HClO_4$ onto mercury microelectrodes. The adsorption thermodynamics follow the Langmuir isotherm over the concentration range from 2×10^{-8} M to 8×10^{-7} M. The same limiting surface coverage, Γ_s ($1.0 \pm 0.08 \times 10^{-10}$ mol cm^{-2}), and energy parameter, β ($5.5 \pm 0.7 \times 10^6$ M^{-1}), are observed for both anthraquinones. The cyclic voltammetry of these single component monolayers is nearly ideal, and the potential dependence of the redox composition follows the Nernst equation with the expected theoretical slope. Microsecond time scale chronoamperometry has been used to probe both the rate of heterogeneous electron transfer to the adsorbed anthraquinone moieties and their surface coverages. Binary monolayers have been formed by simultaneous adsorption of both anthraquinones. A plot of the differential capacitance versus the applied potential exhibits a capacitance minimum at the potential of zero charge, −0.300 V. The film capacitance is estimated to be 30 ± 5 μF cm^{-2}. The surface pK_a of the sulfonic acid groups has been estimated as 2.9 ± 0.5 by measuring the interfacial capacitance as the solution pH is systematically varied. The formal potentials of 2,6-AQDS and 1,5-AQDS are almost identical. Therefore, binary monolayers containing both species exhibit only a single voltammetric peak. Under these circumstances, traditional electroanalytical techniques cannot be used to determine the surface coverages of the individual species. However, in short time scale potential step experiments, three single exponential current decays are separated on a microsecond time scale. These decays correspond to double layer charging and heterogeneous electron transfer to the 2,6-AQDS and 1,5-AQDS redox centers, respectively. This kinetic separation of the Faradaic responses allows the surface coverages of the individual components within the monolayer to be determined. Despite their identical formal potentials, the concentrations of the two anthraquinones in solution have been determined by combining information about heterogeneous kinetics and adsorption thermodynamics.

The objective in forming monomolecular films using self-organization techniques is to produce modified surfaces with well-defined properties.[1] Considerable effort has been devoted to investigating the various aspects of monolayer formation, structure, and molecular orientation, for monolayers containing a single redox active component.[2] However, the structure and dynamics of multicomponent assemblies in which all species are electroactive, have not received the same attention.[3] In this paper, the formation of single component and binary monolayers by the spontaneous adsorption or coadsorption of anthraquinone-2,6-disulfonic acid (2,6-AQDS) and anthraquinone-1,5-disulfonic acid (1,5-AQDS), onto the surface of mercury microelectrodes, is reported. Supramolecular assemblies of this type seek to model photochemical and biological systems where the electron transfer reactions of quinone and hydroquinone compounds play important roles.[4] However, the direct electrochemical investigation of the overall electron and proton transfer mechanism involved in the quinone/hydroquinone reaction is complicated by the rapid nature of the processes involved.[5] Despite this difficulty, Xu recently probed the kinetics and mechanism of surface reactions involving anthraquinone monolayers in considerable detail.[6] This careful study demonstrated that heterogeneous electron transfer occurs on a microsecond time scale, and that the associated rate constant depends on the structure of the anthraquinone. For example, the heterogeneous electron transfer rate constant for 2,6-AQDS monolayers was more than 50 times larger than that for 1,5−AQDS monolayers. This surprisingly large difference in electron transfer rates was attributed to different film structures, and extents of hydrogen bonding, for the two systems.

Quinonoid monolayers and films immobilized on electrode surfaces have been investigated previously.[7] However, past reports have primarily focused on general

[⊗] Abstract published in *Advance ACS Abstracts,* May 15, 1995.

(1) (a) Nuzzo, R. G.; Dubois, L. H.; Allara, D. L. *J. Am. Chem. Soc.* **1990**, *112*, 558. (b) Chidsey, C. E. D.; Loiacono, D. N. *Langmuir* **1990**, *6*, 682. (c) Finklea, H. O.; Snider, D. A.; Fedik, J. *Langmuir* **1990**, *6*, 371. (d) Chidsey, C. E. D. *Science* **1991**, *251*, 919. (e) Hickman, J. J.; Ofer, D.; Zhou, C.; Wrighton, M. S.; Laibinis, P. E.; Whitesides, G. M. *J. Am. Chem. Soc.* **1991**, *113*, 1128. (f) Duevel, R. V.; Corn, R. M. *Anal. Chem.* **1992**, *64*, 337. (g) Murray, R. W. In *Molecular design of Electrode Surfaces*; Murray, R. W., Ed.; Wiley: New York, 1992; Chapter 1.

(2) (a) Ulman, A. *An Introduction to Ultrathin Organic Films From Langmuir–Blodgett to Self-Assembly*, Academic Press: United Kingdom, 1991. (b) Porter, M. D.; Bright, T. B.; Allara, D. L.; Chidsey, C. E. D. *J. Am. Chem. Soc.* **1987**, *109*, 3559. (c) Dubois, L. H.; Zegarski, B. R.; Nuzzo, R. G. *J. Am. Chem. Soc.* **1990**, *112*, 570. (d) Putvinski, T. M.; Schilling, M. L.; Katz, H. E.; Chidsey, C. E. D. *Langmuir* **1990**, *6*, 1567. (e) Laibinis, P. E.; Hickman, J. J.; Wrighton, M. S.; Whitesides, G. M. *Science*, **1989**, *245*, 845. (f) Whitesides, G. M.; Laibinis, P. E. *Langmuir* **1990**, *6*, 87.

(3) Forster, R. J.; Faulkner, L. R. *Anal. Chem.* **1995**, *67*, 1232.

(4) (a) Chambers, J. Q In *The Chemistry of Quinonoid Compounds;* Patai, S.; Rappoport, Z., Eds.; Wiley: New York, 1988; Vol. 11, Chapter 12. (b) Inoue, H.; Hida, M. *Bull. Chem. Soc. Jpn.* **1982**, *55*, 1880. (c) Keita, B.; Nadjo, L. *J. Electroanal. Chem.* **1984**, *163*, 171.

(5) Chen, X.; Zhuang, J.; He, P. *J. Electroanal. Chem.* **1989**, *271*, 257.

(6) Xu, C. Ph.D. Thesis, University of Illinois at Urbana–Champaign, 1992.

(7) (a) He, P.; Crooks, R. M.; Faulkner, L. R. *J. Phys. Chem.* **1990**, *94*, 1135. (b) Soriaga, M. P.; Hubbard, A. T. *J. Am. Chem. Soc.* **1982**, *104*, 2735. (c) Zhang, J.; Anson, F. C. *J. Electroanal. Chem.* **1992**, *331*, 945. (d) Soriaga, M. P.; Hubbard, A. T. *J. Am. Chem. Soc.* **1982**, *104*, 3937. (e) Wipf, D. O.; Wehmeyer, K. R.; Wightman, R. M. *J. Org. Chem.* **1986**, *51*, 4760. (f) Brown, A. P.; Anson, F. C. *J. Electroanal. Chem.* **1978**, *92*, 133. (g) Gamage, R. S. K. A.; McQuillan, A. J.; Peake, B. M. *J. Chem. Soc. Faraday Trans.* **1991**, *87*, 3653. (h) Hillman, A. R. In *Electrochemical Science and Technology of Polymers*; Linford, R. G., Ed.; Elsevier: Amsterdam, 1987; Vol. 1, Chapter 5, p 103.

0743-7463/95/2411-2247$09.00/0

electrochemical and spectroscopic properties of single component systems. This paper focuses on the use of high-speed chronoamperometry to probe the structure and dynamics of mercury microelectrodes modified with binary monolayers. The voltammetric properties of these quinonoid superstructures are nearly ideal at low pH, making them useful model systems for investigating the effect of surface confinement on electron transfer dynamics. The kinetic homogeneity of the redox centers has been probed by monitoring the current response after a potential step designed to alter the redox composition of the monolayer is applied, and by comparing the surface coverages obtained from high-speed chronoamperometry and cyclic voltammetry.

Binary monolayers containing both 2,6-AQDS and 1,5-AQDS have been formed by simultaneous coadsorption of the two compounds onto mercury microelectrodes. By varying the ratio of the two anthraquinones in solution, modified surfaces with a wide range of compositions can be assembled. This synthetic approach is likely to offer much finer control over the properties of the final monolayer than that achievable using single component systems. The overall electrochemical response of these binary monolayers remains close to that expected for an ideal electrochemical reaction involving surface confined redox centers.[8] The effect of coimmobilization on the heterogeneous electron transfer rate constant, k, has been probed using chronoamperometry conducted on a microsecond time scale. That k is approximately independent of the ratio of the two anthraquinones within the film suggests that either lateral interactions between the two types of redox center are weak or there is macroscopic phase separation. Beyond probing the redox properties, the effect of systematically varying the solution pH on the interfacial capacitance has been investigated. In this way, the pK_a of the surface confined sulfonic acid groups has been determined.

In the case of electroactive monolayers that are immobilized on electrode surfaces, the integrated charge under the voltammetric wave is usually taken as a measure of the surface coverage. However, in order for this approach to be applicable to multicomponent systems, the formal potentials of the different constituents must be separated by several tens of millivolts. This requirement is not satisfied for the binary monolayers considered here since the formal potential for the quinone/hydroquinone redox reaction is the same in the two derivatives. Therefore, a different strategy is proposed which separates the Faradaic responses based on differences in the kinetic properties of the two anthraquinone redox centers. The possibility of extending this kinetic approach to determine bulk concentrations in solution by combining information about adsorption thermodynamics and surface coverage is also considered.

Experimental Section

Apparatus. Electrochemical cells were of conventional design and were thermostated within ±0.2 °C using a Julabo F10-HC refrigerated circulating bath. All potentials are quoted with respect to a BAS Ag/AgCl gel-filled reference electrode, the potential of which was 35 mV more positive than that of the saturated calomel electrode (SCE). In order to prevent chloride contamination from the reference electrode, the electrolytic solution was separated from the reference electrode by a salt bridge filled with saturated KNO_3. Cyclic voltammetry was performed using an EG&G model 273 potentiostat/galvanostat and a conventional three-electrode cell. All solutions were degassed using nitrogen, and a blanket of nitrogen was maintained over the solution during all experiments.

As described previously, a custom built function generator–potentiostat, which had a rise time of less than 10 ns, was used to apply potential steps of variable pulsewidth and amplitude directly to a two-electrode cell.[9] A Pt foil and an Ag/AgCl reference electrode were combined to form a counter electrode. The foil lowered the resistance and provided a high-frequency path.

Microelectrodes were fabricated from platinum microwires (Goodfellow Metals Ltd.) of radii between 5 and 25 μm by sealing them in soft glass using a procedure described previously.[6,10] Microdisk electrodes were exposed by removing excess glass using 600 grit emery paper followed by successive polishing with 12.5, 5, 1, 0.3, and 0.05 μm alumina. The polishing material was removed between changes of particle size by sonicating the electrodes in deionized water for at least 5 min. The polished electrodes were electrochemically cleaned by cycling in 0.1 M $HClO_4$ between potential limits chosen to first oxidize and then to reduce the surface of the platinum electrode. Finally, the electrode was cycled between −0.300 and 0.700 V in 0.1 M $NaClO_4$ until hydrogen desorption was complete.

Mercury hemispherical microelectrodes, which were used exclusively in the experiments reported here, were formed by electrodeposition of mercury onto platinum electrodes that were prepared as described above. The deposition solution contained 6 mM mercurous nitrate, 0.5% HNO_3, and 1.0 M KNO_3. Sufficient charge was passed at 0.000 V to form a mercury droplet on the platinum surface whose radius was at least twice as large as that of the platinum microwire.[11] The area of these mercury microelectrodes was determined from cyclic voltammetry and chronocoulometry using $[Os(2,2'\text{-bipyridyl})_2Cl_2]^{2+}$ as a solution phase electrochemical probe.[12] Electrode areas were in the range from 3×10^{-6} to 2×10^{-5} cm^2. RC cell time constants measured in blank electrolyte solution were between 50 and 500 ns, depending on the electrode radius and the supporting electrolyte concentration. The interfacial kinetics were measured only at times greater than about 5-10 RC.

Materials and Procedures. The disodium salts of anthraquinone-2,6–disulfonic acid (2,6-AQDS) and anthraquinone-1,5-disulfonic acid were obtained from Aldrich Chemical Co. They were recrystallised from purified water three times using decolorizing charcoal. The recrystallization and subsequent storage were carried out in the dark to avoid photochemical decomposition.

Unless stated otherwise, the supporting electrolyte was aqueous 1.0 M $HClO_4$. Water was purified using a Milli-Q filtering system (Millipore). Monolayers were formed by immersing the mercury microelectrodes in the supporting electrolyte solution containing the anthraquinone of interest at the desired concentration. All subsequent measurements on the monolayers were performed with this concentration of anthraquinone present in solution. The highest solution concentration was in the micromolar range, which means that the maximum contribution from diffusion to the overall current observed in chronoamperometry or cyclic voltammetry is less than 5%. The time evolution of the surface coverage was monitored using cyclic voltammetry until the equilibrium surface coverage was attained.

Binary monolayers were formed by immersing the microelectrode in an electrolytic solution containing both anthraquinones. The ratio of 2,6-AQDS to 1,5-AQDS within the monolayers was controlled by altering the concentrations of the two anthraquinones in solution. The solution concentration ratio of the competing adsorbates was varied from 0.9 to 0.1 to produce monolayers with a range of compositions.

Results and Discussion

General Electrochemical Properties of Single Component Monolayers. First, the electrochemical

(8) (a) Laviron, E. *J. Electroanal. Chem.* **1974**, *52*, 395. (b) Brown, A. P.; Anson, F. C. *Anal. Chem.* **1977**, *49*, 1589.

(9) Walsh, M. R. Ph. D. Thesis, University of Illinois at Urbana–Champaign, 1988.

(10) Faulkner, L. R.; Walsh, M. R.; Xu, C. In *Contemporary Electroanalytical Chemistry*, Ivaska, A. Ed., Plenum Press, New York, 1990; p 5.

(11) Wightman, R. M.; Wipf, D. O. *Electroanalytical Chemistry*; Bard, A. J., Ed.: Marcel Dekker: New York, 1989; Vol. 15.

(12) Forster, R. *Chem. Soc. Rev.* **1994**, *23*, 289.

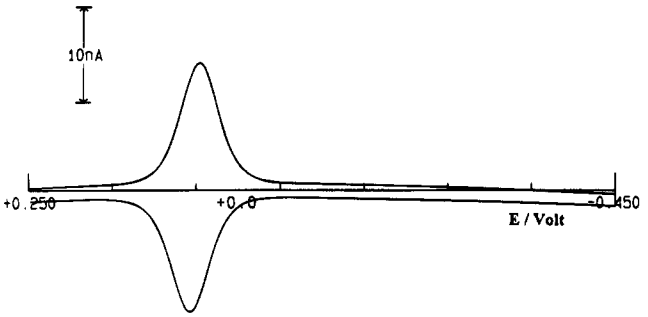

Figure 1. Cyclic voltammogram for a 10 μm radius mercury microelectrode immersed in a 10 μM solution of 2,6-AQDS in 1.0 M $HClO_4$. The scan rate is 10 V/s. Cathodic currents are up; anodic currents are down. The initial potential is −0.450 V.

Scheme 1

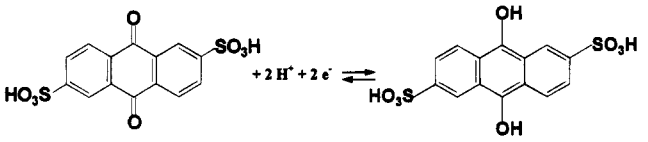

behavior of monolayers that contain a single type of anthraquinone species is reported. Unless stated otherwise, representative behavior for both systems is illustrated using data for either 2,6-AQDS or 1,5-AQDS. Figure 1 shows a representative cyclic voltammogram for a 10 μm mercury microelectrode immersed in a 10 μM solution of 2,6-AQDS in 1.0 M $HClO_4$. This voltammogram is consistent in all respects with that expected for an electrochemically reversible reaction involving a surface-confined species.[8] For example, the peak shapes are independent of scan rate at least over the range 0.1−20 V/s, and the peak height scales linearly with the scan rate, v, unlike the $v^{1/2}$ dependence expected for a freely diffusing species.[13] Therefore, it appears that the anthraquinone adsorbs onto the surface of the mercury microelectrode to give an electroactive film. Where there are no lateral interactions between adsorbates and a rapid equilibrium is established with the electrode, a zero-peak-to-peak splitting and an FWHM of 45.3 mV are expected for a reaction in which two electrons are transferred.[8] Therefore, in agreement with previous reports,[6,7a] Figure 1 suggests that the overall redox reaction involves transfer of two electrons and two protons to surface immobilized anthraquinone moieties (Scheme 1).

The electrochemical behavior of the adsorbed species can be further probed by determining the redox composition as a function of the applied potential. For an ideal system involving transfer of two electrons, the ratio of oxidized to reduced species should change by approximately 1 order of magnitude for each 29.5 mV change in the applied potential about the formal potential $E^{o\prime}$.[13] Chronocoulometry can be successfully applied to modified electrodes to determine the redox composition as the applied potential is systematically varied.[14] In the experiments reported here, the potential was stepped in a positive direction from a potential 100 mV more negative than $E^{o\prime}$ using a pulse amplitude, E_{amp}. Initially E_{amp} was 10 mV, and it was increased by 10 mV between successive experiments until the potential was stepped to a value 100 mV more positive than $E^{o\prime}$. By measuring the charge passed in each of these steps and determining the charge passed in an exhaustive electrolysis experiment, the

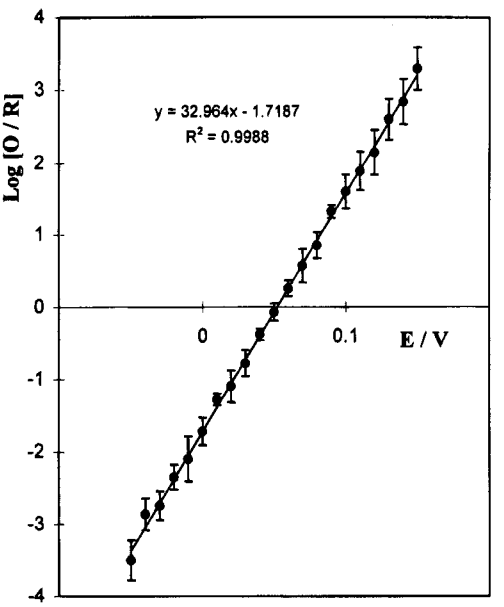

Figure 2. The redox composition of a 1,5-AQDS monolayer as a function of the potential. The supporting electrolyte is aqueous 1.0 M $HClO_4$.

functional relationship between the ratio of the oxidized to reduced forms of the anthraquinone and the applied potential could be probed. Figure 2 illustrates representative data for a 1,5-AQDS film. The slope of this plot, 33 ± 2 mV/decade, is indistinguishable from that predicted for a two-electron transfer reaction by the Nernst equation,[13] confirming that the electrochemical response of these films is nearly ideal under the experimental conditions employed.

Adsorption Isotherms. After correcting for the contribution from double layer charging, the total charge withdrawn or injected to oxidize or reduce the layer can be determined from the area under the voltammetric peaks. From the charge under the wave and the geometric electrode area, the surface coverage of anthraquinone molecules can be established. To define the adsorption isotherm, the surface coverages of 2,6-AQDS or 1,5-AQDS at equilibrium were determined as the solution concentration was systematically varied. Figure 3 shows the change in surface coverage as the solution concentration of 2,6-AQDS or 1,5-AQDS is varied from 2×10^{-8} to 9×10^{-7} M. The Langmuir isotherm[13,15] describes equilibrium adsorption where lateral interactions between the adsorbed molecules are absent, and the limiting surface coverage is dictated simply by the size of the adsorbate. The essentially ideal voltammetric response shown in Figure 1 suggests that the Langmuir isotherm may be an appropriate description of adsorption in these systems. This isotherm is described by the following expression:[13,15]

$$\Gamma_i/(\Gamma_s-\Gamma_i) = \beta_i C_i \qquad (1)$$

where Γ_i is the surface excess of species i at equilibrium, Γ_s is the surface excess of species i at saturation, β_i is the energy parameter, and C_i is the concentration of species i in solution. In the following discussions activity effects are incorporated into the energy parameter. The lines shown in Figure 3 are the best fits to the experimental data provided by the Langmuir isotherm, confirming that satisfactory agreement between experiment and theory is obtained.

(13) Bard, A. J.; Faulkner, L. R. *Electrochemical Methods: Fundamentals and Applications*; Wiley: New York, 1980.
(14) (a) Forster, R. J.; Faulkner, L. R. *J. Am. Chem. Soc.* **1994**, *116*, 5444. (b) Forster, R. J.; Faulkner, L. R. *J. Am. Chem. Soc.* **1994**, *116*, 5453. (c) Forster, R. J.; Vos, J. G. *Langmuir* **1994**, *10*, 4330.
(15) (a) Laviron, E. *Electroanal. Chem.* **1982**, *12*, 53. (b) Trassatti, S. *J. Electroanal. Chem.* **1974**, *53*, 335.

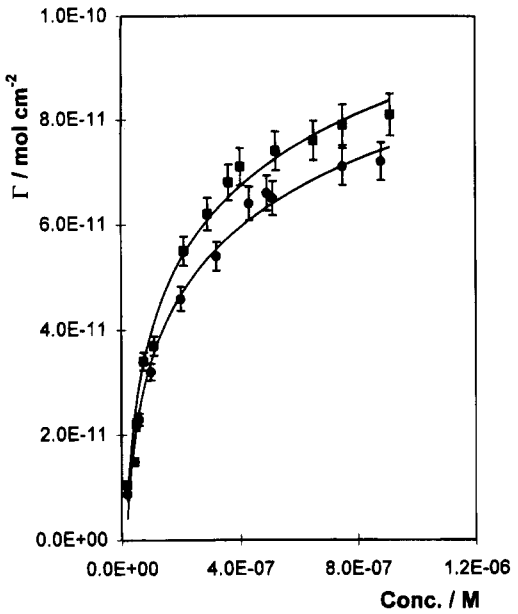

Figure 3. Relationship between the surface coverage of 2,6-AQDS (●), and 1,5-AQDS (■), and their bulk concentrations. The supporting electrolyte is 1.0 M $HClO_4$.

The Langmuir isotherm predicts that a plot of C_i/Γ_i vs C_i should be linear and that the saturation surface coverage and the energy parameter can be obtained from the slope and intercept, respectively. In all cases, plots of this type were linear (correlation coefficients > 0.995) for both 2,6-AQDS and 1,5-AQDS films. Modeling the experimental data using a Frumkin isotherm,[13,15] which considers adsorbate–adsorbate interactions, gave interaction parameters that were close to zero. This observation suggests that attractions or repulsions between adsorbates exert little influence over the thermodynamics of adsorption. The values of Γ_s provided by the Langmuir isotherm for the two types of layer were experimentally indistinguishable, with values of $1.0 \pm 0.08 \times 10^{-10}$ and $9.9 \pm 0.06 \times 10^{-11}$ mol cm^{-2} being observed for the 2,6 and 1,5 derivatives, respectively. This limiting surface coverage corresponds to an average area of occupation per molecule of approximately 185 Å^2. This value is consistent with the range found by Faulkner and coworkers for monolayer coverages[7a] (190–210 Å^2), but is distinctly larger than the 130 Å^2 indicated by the work of Soriaga and Hubbard for a flat orientation on platinum.[7b] This difference in the area of occupation has been interpreted in terms of differences in the surface bonding at platinum and mercury.[16] Therefore, it appears that dense monolayers form when mercury microelectrodes are immersed in solutions containing anthraquinonedisulphonate at concentrations greater than about 1 μM.

The energy parameters for these systems are also experimentally indistinguishable and have values of $5.2 \pm 0.7 \times 10^6$ M^{-1} and $5.9 \pm 0.5 \times 10^6$ M^{-1}, for 2,6–AQDS and 1,5-AQDS, respectively. That the formal potentials, peak widths, and strengths of adsorption are essentially identical for these two anthraquinones suggests that the thermodynamics of adsorption, and lateral interactions, are similar in both circumstances.

In the following section, data on the rate of heterogeneous electron transfer, as determined using high-speed chronoamperometry, is reported. The ultimate objective is to compare the rate constants obtained for single component systems with those obtained for mixed structures. Moreover, the ability of chronoamperometry to determine anthraquinone surface coverages within single component monolayers is considered before dealing with more complex systems.

(16) Soriaga, M. P.; Binamira-Soriaga, E.; Hubbard, A. T.; Benziger, J. B.; Pang, K.-W. P. *Inorg. Chem.* **1985**, *24*, 65.

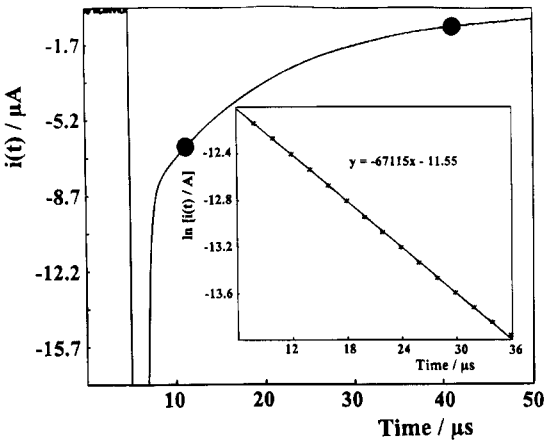

Figure 4. Current response for a 16 μm radius mercury microelectrode immersed in a 10 μM solution of 2,6-AQDS following a potential step from −0.200 to 0.100 V. The supporting electrolyte is 1.0 M $HClO_4$. The inset shows the semilog plot for data between the marks on the current–time transient. The time axis on the inset is referenced to the leading edge of the potential step.

Chronoamperometry. For an ideal electrochemical reaction involving a surface bound species, the Faradaic current following a potential step that changes the redox composition of the monolayer exhibits a single exponential decay in time according to:[13,14ab,17]

$$i_F(t) = kQ \exp(-kt) \qquad (2)$$

where k is the apparent rate constant for the overall reaction and Q is the total charge passed in the redox transformation.

Figure 4 shows the current response for a dense 2,6-AQDS monolayer following a potential step from −0.200 V to a potential E of 0.100 V. This potential step corresponds to an overpotential ($\eta \equiv E - E^{o\prime}$) of 50 mV. Figure 4 shows that two current decays, corresponding to double layer charging and Faradaic current flow, respectively, are separated on a 50 μs time scale. These two processes are time-resolved because the time constant for double layer charging is much smaller than that of the Faradaic reaction. In this study, the electron transfer dynamics are only probed under those circumstances where the time constant of double layer charging is at least 5 times shorter than that of the Faradaic reaction.

The linearity of the semilog plot shown in the inset of Figure 4 indicates that heterogeneous electron transfer associated with oxidation of the 2,6-AQDS monolayer is a first-order process. The unusual linearity also indicates that a single rate constant predominates over the time required to collect more than 95% of the total Faradaic charge. This observation is significant and contrasts with pure ferrocene alkanethiol monolayers where a heterogeneous distribution of rate constants is observed, and diluent electroinactive spacer molecules must be added to obtain monodisperse behavior.[18] The predominance of

(17) Finklea, H. O.; Hanshew, D. D. *J. Am. Chem. Soc.* **1992**, *114*, 3173.

(18) (a) Chidsey, C. E. D. *Science* **1991**, *251*, 919. (b) Chidsey, C. E. D.; Bertozzi, C. R.; Putvinski, T. M.; Mujsce, A. M. *J. Am. Chem. Soc.* **1990**, *112*, 4301. (c) De Long, H. C.; Donohue, J. J.; Buttry, D. A. *Langmuir* **1991**, *7*, 2196. (d) Donohue, J. J.; Buttry, D. A. *Langmuir* **1988**, *4*, 671. (e) Weber, K.; Creager, S. E. *Anal. Chem.* **1994**, *66*, 3164. (f) Tender, L.; Carter, M. T.; Murray, R. W. *Anal. Chem.* **1994**, *66*, 3173.

Table 1. Cyclic Voltammetric Surface Coverages, Γ(CV), Heterogeneous Electron Transfer Rate Constants, k, and Surface Coverages As Determined by High-Speed Chronoamperometry, Γ(CA), for Single Component 2,6-AQDS and 1,5-AQDS Monolayers[a]

2,6-AQDS			1,5-AQDS		
$10^{11}\Gamma$(CV)/mol cm^{-2} [b]	$10^{-4}k$/s^{-1} [c]	$10^{11}\Gamma$(CA)/mol cm^{-2} [d]	$10^{11}\Gamma$(CV)/mol cm^{-2} [b]	$10^{-3}k$/s^{-1} [c]	$10^{11}\Gamma$(CA)/mol cm^{-2} [d]
0.88(0.02)	4.6(0.2)	0.98(0.04)	1.05(0.06)	0.84(0.03)	1.20(0.08)
1.77(0.04)	4.7(0.3)	1.86(0.08)	2.25(0.05)	0.86(0.04)	2.37(0.16)
2.21(0.05)	5.2(0.3)	2.56(0.14)	3.02(0.13)	0.90(0.05)	3.38(0.23)
3.15(0.04)	5.3(0.3)	3.65(0.15)	3.85(0.16)	0.90(0.03)	4.21(0.17)
4.63(0.03)	5.6(0.3)	5.23(0.26)	5.35(0.26)	0.92(0.04)	6.03(0.23)
5.63(0.08)	5.7(0.2)	6.30(0.32)	6.07(0.34)	0.90(0.03)	6.83(0.38)
6.20(0.09)	5.8(0.3)	6.76(0.33)	6.73(0.32)	0.94(0.02)	7.52(0.42)
6.43(0.12)	6.3(0.3)	7.21(0.28)	7.20(0.36)	0.97(0.05)	7.19(0.41)
6.52(0.11)	6.3(0.3)	7.04(0.41)	7.56(0.34)	1.00(0.03)	7.47(0.35)
7.08(0.14)	6.6(0.3)	7.87(0.39)	7.76(0.20)	1.10(0.04)	7.61(0.51)
7.29(0.15)	6.7(0.2)	8.16(0.41)	8.00(0.23)	1.08(0.05)	8.21(0.34)

[a] Numbers in parentheses represent the standard deviations for measurements on at least three individual monolayers. [b] Surface coverages determined from the area under the cyclic voltammetric peak. [c] The overpotential is 50 mV with respect to the formal potential of the quinone/hydroquinone redox reaction. [d] Surface coverage determined using high speed chronoamperometry. See the text for details.

a single rate constant for these anthraquinone monolayers suggests either that there is largely a single microenvironment (electron transfer distance, and reorganization energy) within the monolayer or that there is very rapid interconversion between dissimilar sites.

The presence of only weak lateral interactions in these anthraquinone films is probably the primary reason why nearly ideal electrochemical responses are observed. However, it is perhaps useful to consider how differences in the monolayer charge density between ferrocene alkanethiol monolayers and these anthraquinone systems might influence the electrochemical responses. That electron transfer is coupled to proton transfer in the structures considered here means that both the initial and final states, before and after oxidation of the monolayer, are uncharged. This situation contrasts with other redox active monolayers where a layer of charge compensating counterions must be assembled in solution when the monolayer is oxidized. Under those circumstances, the charge density of the monolayer changes continuously as heterogeneous electron transfer proceeds. This variation may cause the reaction free energy to change throughout the reaction, causing a multiexponential decay of the Faradaic current to be observed.[19,20] If electron and proton transfer are concerted in these anthraquinone monolayers, then the monolayer is uncharged throughout the redox transformation, perhaps contributing to the unusually linear responses shown in Figure 4.

As indicated by eq 2, the absolute slope of the linear regression line for the semilog plot of Figure 4 represents the heterogeneous electron transfer rate k. The value obtained, 6.7×10^4 s^{-1} confirms the rapid nature of electron and proton transfer within these superstructures. Table 1 shows the variation of the heterogeneous rate constant measured at $\eta = 50$ mV as the surface coverage is systematically varied. These data show that the interfacial kinetics are approximately independent of the surface coverage with k increasing by less than 30% as the surface coverage is changed from approximately 1×10^{-11} to 8×10^{-11} mol cm^{-2}. Since the heterogeneous electron transfer rate depends exponentially on the separation of the electronic manifolds on the two sides of the interface,[21] the insensitivity of k to changes in the surface coverage suggests that the average electron transfer distance does not depend on the coverage. This observation may indicate that partial monolayers form as dense islands separated by regions in which the mercury surface is unmodified, or that the molecular orientation does not depend on the packing density. Future publications will address these possibilities using surface sensitive spectroscopy.

Table 1 confirms the observation made by Xu that the heterogeneous electron transfer rate for 1,5-AQDS monolayers is about 50 times smaller than that found for 2,6-AQDS systems.[6] Xu attributes this surprisingly large difference in electron transfer dynamics to differences in film structure and extents of hydrogen bonding. The ultimate objective of this paper is to probe the possibility that this large difference in heterogeneous rate constant can be exploited to determine the surface coverages of both anthraquinones within binary structures. Therefore, the origin of this difference in electrode kinetics is not examined any further here. Before considering multicomponent assemblies, the ability of high-speed chronoamperometry to determine surface coverages within single component monolayers is reported.

The intercept of the semilog plot in Figure 4 represents the product ln (kQ), allowing the charge passed in the redox transformation to be determined.[14a,b] As demonstrated by Figure 2, an overpotential of 50 mV decreases the number of reduced species within the monolayer to less than 3% of the total. Therefore, this potential step effectively causes complete oxidation of the film, and the full surface coverage can be calculated from the intercept of Figure 4 using the relation[8]

$$\Gamma = Q/nFA \qquad (3)$$

where n is the number of electrons transferred, F is Faraday's constant, and A is the electrode area. The charge obtained from the intercept in the semilog plot of Figure 4 is 1.43×10^{-10} C, which corresponds to a surface coverage of 9.2×10^{-11} mol cm^{-2}, given that the electrode area is 8.0×10^{-6} cm^2. This value is within 10% of that found by cyclic voltammetry.

Table 1 contains surface coverages determined by both cyclic voltammetry Γ(CV), and chronoamperometry Γ(CA), for single component monolayers containing 2,6-AQDS or 1,5-AQDS alone. That the surface coverages determined by cyclic voltammetry and chronoamperometry agree with one another to within 15% over this range confirms that high-speed chronoamperometry can be successfully used to determine surface coverages of redox species within single component monolayers. This agreement also indicates that all of the surface confined molecules are redox active on a microsecond time scale; i.e., relatively few if any sites are kinetically isolated. Table

(19) Smith, C. P.; White, H. S. *Anal. Chem.* **1992**, *64*, 2398.
(20) Creager, S. E.; Weber, K. *Langmuir* **1993**, *9*, 844.
(21) (a) Li, T. T.-T.; Weaver, M. J. *J. Am. Chem. Soc.* **1984**, *106*, 6107. (b) Miller, C.; Cuendet, P.; Grätzel, M. *J. Phys. Chem.* **1991**, *95*, 877. (c) Miller, C.; Grätzel, M. *J. Phys. Chem.* **1991**, *95*, 5225.

1 also shows that the between monolayer deviation is similar for the two techniques, demonstrating the ability of microelectrodes to provide high-quality analytical information at short times.[12]

Mixed Monolayers. It is clear that in order to perform increasingly more demanding tasks using modified electrodes, more complex structures will have to be constructed in which the architecture is controlled at the molecular level. With this objective in mind, the remainder of this paper deals with the properties of binary monolayers formed by the simultaneous coadsorption of both 2,6-AQDS and 1,5-AQDS.

Interfacial Capacitance. Probing the double layer capacitance C_{dl} gives an insight into the change in interfacial charge distribution that accompanies monolayer formation, the relative perfection of the monolayer, and perhaps its thickness.[2b,14,22,23] In this study, small amplitude potential step chronoamperometry has been used to measure the interfacial capacitance as the applied potential, or the solution pH, was systematically varied. The pulse amplitude employed was 25 mV, which is sufficiently small so that the measured capacitance can be regarded as an approximate differential capacitance.[13]

In experiments designed to probe the potential dependence of C_{dl}, the potential was stepped from an initial value E_i using a pulse amplitude of 25 mV, and the resulting current transient was recorded and analyzed. Between successive experiments, E_i was increased monotonically by 25 mV from −0.700 to 0.250 V. Stepping the potential in a region where the redox composition of the monolayer did not change, i.e., far from $E^{\circ\prime}$, gave only a single exponential current decay corresponding to double layer charging.[11,13] Stepping the potential close to $E^{\circ\prime}$ gave three well-defined single exponential current decays. These transients correspond to double layer charging and heterogeneous electron transfer to the two types of anthraquinone center. These multiple decay responses are discussed in greater detail later.

In experiments designed to probe the pH dependence of C_{dl}, the potential was stepped in a region where the film was electroinactive, and only a single exponential decay due to double layer charging was observed.

In both cases, the capacitive current was analyzed using a plot of ln $i(t)$ vs t. The resistance R_u and approximate double layer capacitance C_{dl} were determined using eq 4[11,14]

$$i_c(t) = (\Delta E/R_u)\exp(-t/R_uC_{dl}) \qquad (4)$$

where ΔE is the pulse amplitude.

First, the dependence of the interfacial capacitance on potential is reported for a binary monolayer formed from a 0.05 M $NaClO_4$ solution containing 10 μM 2,6-AQDS and 10 μM 1,5-AQDS. The pH of this solution (5.5) is expected to be sufficiently high to fully deprotonate the sulfonic acid groups, yet is below the pK_a of the phenolic protons (7.35).[24] Therefore, the monolayer has a 2− charge at all potentials investigated. Figure 5 illustrates the dependence of the double layer capacitance on potential for this binary monolayer. In plotting these data, each value of C_{dl} is associated with its corresponding initial potential E_i. Figure 5 shows that a shallow minimum in the capacitance is observed at approximately −0.300 V

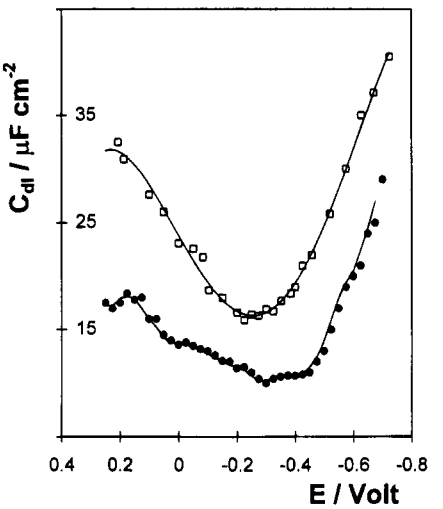

Figure 5. Dependence of the double layer capacitance C_{dl} on the applied potential. ● represents data for a mercury microelectrode immersed in a solution containing 10 μM 2,6-AQDS and 10 μM 1,5-AQDS. □ represents data for a clean mercury microelectrode in the same electrolytic solution but without any dissolved anthraquinone. In both cases the supporting electrolyte is 0.05 M $NaClO_4$ at a pH of approximately 5.5. Capacitance values are reproducible between monolayers to within ±2 μF cm^{-2}.

for a modified mercury microelectrode. On the basis of the Gouy−Chapman−Stern (GCS) model of the electrochemical double layer,[13,25] a minimum in the capacitance is expected at the potential of zero charge, E_{PZC}. Therefore, these data suggest that when the monolayer is both deprotonated and reduced, E_{PZC} is −0.300 V.

In order to probe the effect of monolayer formation on E_{PZC}, the potential dependence of the interfacial capacitance has been measured for a clean mercury microelectrode in the same electrolytic solution in the absence of anthraquinone adsorption. These data are also illustrated in Figure 5, and they reveal that under these conditions, E_{PZC} for clean mercury is approximately −0.210 V. Therefore, forming a dense anthraquinone assembly at the interface causes E_{PZC} to shift in a negative potential direction by approximately 90 mV. This behavior is expected because monolayer formation involves the specific adsorption of negatively charged anthraquinone molecules at the electrode/solution interface.[13] Adsorption of these anions causes the charge on the solution side of the interface to become nonzero, which must be balanced. Since the electrode is more polarizable than solution, the countercharge is induced there. To regain the condition in which there is no excess charge on the metal, the potential shifts in a negative direction so that the charge due to adsorbed anthraquinones is exactly counterbalanced by an opposing excess charge in the diffuse layer.

For an electrochemical double layer the differential capacitance increases with a decreasing separation between the electrode surface and the plane of closest approach for ionic charge and increases with increasing dielectric constant. In the case of an electrode coated with a monolayer, the total double layer capacitance C_{dl} typically contains contributions from the film C_F, and the solution capacitance C_S.

$$1/C_{dl} = 1/C_F + 1/C_S \qquad (5)$$

Since highly ordered, defect-free monolayers exhibit small interfacial capacitances,[2b] an important objective

(22) Acevedo, D.; Abrûna, H. D. *J. Phys. Chem.* **1991**, *95*, 9590.
(23) Bryant, M. A.; Crooks, R. M. *Langmuir* **1993**, *9*, 385.
(24) (a) Ksenzhek, O. S.; Petrova, S. A.; Oleinik, S. V.; Kokodyashnyi, M. V.; Moskovskii, V. Z. *Elektrokhimiya* **1977**, *13*, 182. (b) Sun, L.; Johnson, B.; Wade, T.; Crooks, R. M. *J. Phys. Chem.* **1990**, *94*, 8869.
(25) Delahay, P. *Double Layer and Electrode Kinetics*; Wiley: New York, 1965.

is to evaluate C_F. One strategy to determine C_F is to measure C_S in the absence of the monolayer and then use eq 5 to subtract this contribution from the value of C_{dl} obtained in the presence of a monolayer. Figure 5 yields values of approximately 16 and 10 μF cm^{-2} for the capacitance at E_{PZC} of a clean mercury surface and an anthraquinone modified interface, respectively. These data suggest that the film capacitance is approximately 27 μF cm^{-2}. However, this analysis assumes that the potential distribution at the bare and modified interfaces are identical. The validity of this assumption will depend on the potential distribution at the modified interface, i.e., whether the potential decays exponentially with increasing distance from the electrode surface, or decays linearly across the monolayer thickness and then exponentially in solution, which will be dictated in part by the permeability of the film to electrolyte and solvent.

Another potentially more fruitful strategy is to make the contribution from solution phase capacitance to the total double layer capacitance negligible.[14c] This may be possible since only the diffuse layer capacitance C_S depends on the concentration of supporting electrolyte. Therefore, if solvent and electrolyte ions do not permeate into the monolayer, the limiting value of C_{dl} at high electrolyte concentration represents the film capacitance C_F. The double layer capacitance experimentally determined at E_{PZC} initially increases with increasing electrolyte concentration before attaining a limiting value of 30 μF cm^{-2}, for supporting electrolyte concentrations above 0.2 M. If this limiting capacitance is dominated by the film capacitance, then assuming a monolayer thickness of 3 Å the relative dielectric constant within the film is estimated as 10. This dielectric constant is considerably less than that of pure water (78.5) and is consistent with the formation of a dense organic monolayer.[2b]

Capacitance data can also be used to probe non-Faradaic processes, e.g., protonation/deprotonation reactions that occur within monolayers as the solution pH is systematically varied. In the model of Smith and White,[26] the pH dependence of the total double layer capacitance C_{dl} is described as follows

$$1/C_{dl} = 1/C_F + 1/[C_S + C(f)] \quad (6)$$

where $C(f)$ represents the variation of the capacitance with extent of monolayer protonation. Therefore, it ought to be possible to determine the surface pK_a of the sulfonic acid side groups by investigating the pH dependence of the interfacial capacitance. Toward this objective, the interfacial capacitance has been probed in a background electrolyte of 0.15 M $NaClO_4$ as the pH of the solution is systematically varied by the addition of concentrated $HClO_4$. This measurement was made at the potential of zero charge for the monolayer (−0.300 V) determined above. The anthraquinone moieties are not redox active at this potential (Figure 1), and the current response following a 25 mV potential step is entirely capacitive in nature. Figure 6 shows the interfacial capacitance observed as the solution pH is systematically varied from 7.0 to 1.0. According to Smith and White's model,[26] at pH values near the pK_a of the immobilized sulfonic acid groups, $C(f)$ reaches a maximum value giving a local maximum in C_{dl}. The general shape of the curve shown in Figure 6 is consistent with Smith and White's theory although the observed capacitance maximum is less than that predicted. The pK_a estimated from the data shown in

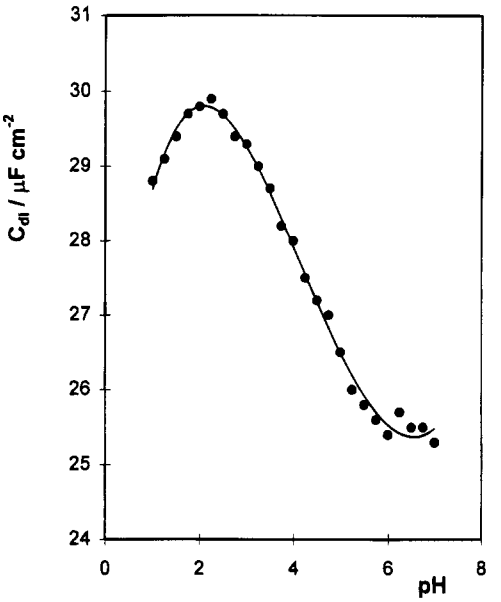

Figure 6. Dependence of the double layer capacitance at −0.300 V on pH for a mercury microelectrode immersed in a 0.15 M $NaClO_4$ solution containing 10 μM 2,6−AQDS and 10 μM 1,5-AQDS. The solution pH was adjusted using concentrated $HClO_4$. Capacitance values are reproducible between monolayers to within ±1 μF cm^{-2}.

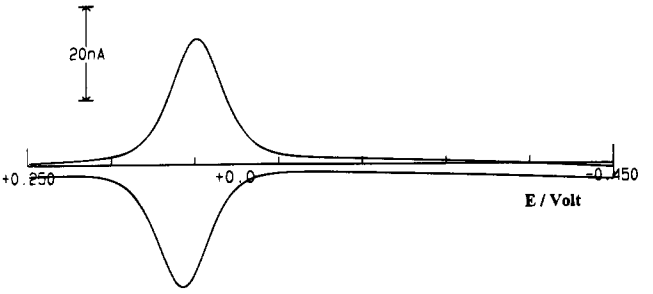

Figure 7. Cyclic voltammogram of a 10 μm radius mercury microelectrode immersed in a 1.0 M $HClO_4$ solution containing 10 μM 2,6-AQDS and 10 μM 1,5-AQDS. The scan rate is 20 V/s. Cathodic currents are up; anodic currents are down. The initial potential is −0.450 V.

Figure 6 is 2.9 ± 0.5.[23,26] This value is approximately 2.5 pH units higher than that reported for anthraquinone-2-sulfonic acid in water.[27] This apparent shift in pK_a may be due to the rather hydrophobic microenvironment of the anthraquinone monolayer.

Redox Properties. Cyclic voltammetry represents a useful technique for measuring the surface coverage of redox active material within monolayers containing a single type of anthraquinone. However, the situation regarding mixed monolayers containing both 2,6-AQDS and 1,5-AQDS is distinctly different. Figure 7 shows that a cyclic voltammogram of a monolayer deposited from a solution containing equimolar concentrations of both 2,6-AQDS and 1,5-AQDS exhibits only a single peak associated with the quinone/hydroquinone redox reaction. It is unlikely that only one of the anthraquinones adsorbs given the similarity of the energy adsorption parameters for the two systems. Chronoamperometry (vide infra) strongly suggests that these monolayers do contain both species. The voltammetric behavior shown in Figure 7 is expected since the formal potentials of the two types of redox center

(26) Smith, C. P.; White, H. S. *Langmuir* **1993**, *9*, 1.

(27) Dean, J. A. *Handbook of Organic Chemistry*; McGraw Hill: New York, 1987.

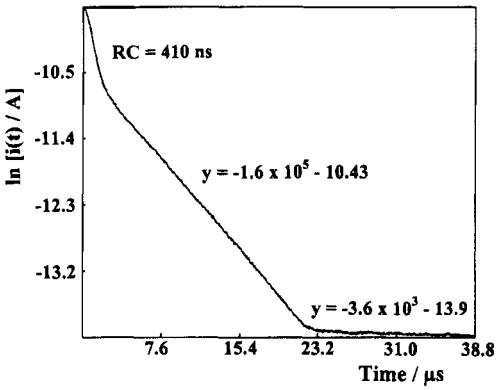

Figure 8. Log current versus time response for a 25 μm radius mercury microelectrode immersed in a solution containing 10 μM 2,6-AQDS and 10 μM 1,5-AQDS following a potential step where the overpotential was 0.106 V. The supporting electrolyte is 1.0 M $HClO_4$. The time axis is referenced with respect to the leading edge of the potential step.

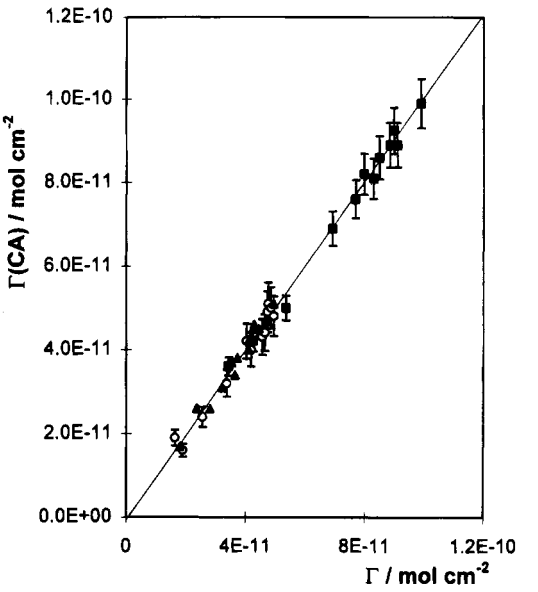

Figure 9. Relationship between the surface coverages Γ predicted by eqs 6 and 7 and those experimentally determined using chronoamperometry, Γ(CA). The total surface coverage of both anthraquinones is denoted by ■, the surface coverage of 2,6-AQDS by ○, and the surface coverage of 1,5-AQDS by ▲. The solid line indicates the behavior expected for a direct, unbiased correlation.

are essentially identical. However, as shown in Table 1, the heterogeneous electron transfer rate constants are not identical for the two types of redox center, at least not in single component monolayers. Therefore, the possibility exists that differences in the heterogeneous electron transfer rates to the two anthraquinone derivatives could be exploited to determine their respective surface coverages.[3]

Figure 8 shows a semilog plot for this binary monolayer following a potential step from −0.200 to 0.150 V. This potential step oxidizes both the 2,6-AQDS and 1,5-AQDS centers within the monolayer. The most striking feature of Figure 8 is that three single exponential decays are separated on a 40 μs time scale. These three processes correspond to double layer charging and oxidation of the two types of anthraquinone molecules within the supramolecular assembly.[3,13] When an identical overpotential is applied, the rate constants obtained from the second and third decays of Figure 8 are within 10% of those found for single component monolayers of 2,6-AQDS and 1,5-AQDS, respectively. Observation of the same heterogeneous electron transfer rate constants for binary and pure monolayers suggests that lateral electron transfer between adjacent 2,6-AQDS and 1,5-AQDS molecules does not occur to any great extent and that heterogeneous electron transfer is the primary mechanism by which the redox composition of these mixed monolayers is changed.

The surface coverages obtained from the intercepts of the semilog plots using eq 3 are $4.9 \pm 0.2 \times 10^{-11}$ and $5.5 \pm 0.3 \times 10^{-11}$ mol cm^{-2} for the 2,6-AQDS and 1,5-AQDS redox centers, respectively. Given that the concentrations of the two anthraquinones in solution are identical, and that the energy parameters of adsorption are very similar, one would expect this binary monolayer to contain equal coverages of the 2,6 and 1,5 derivatives. It is important to note that the total surface coverage of anthraquinone, $1.0 \pm 0.5 \times 10^{-10}$ mol cm^{-2}, is indistinguishable from that found for dense monolayers containing only 2,6-AQDS or 1,5-AQDS. These observations strongly suggest that high-speed chronoamperometry can be used to determine surface coverages within binary monolayers even though the formal potentials of the two components are identical. The only requirement of this approach is that the interfacial kinetics of the individual components be sufficiently different so that single exponential decays are observed.

Competitive Adsorption. The Langmuir isotherm[13,16] can be used to describe competitive adsorption of species i and j according to the following relations:

$$\Gamma_i = \Gamma_{i,s}\beta_i C_i/(1 + \beta_i C_i + \beta_j C_j) \quad (6)$$

$$\Gamma_j = \Gamma_{j,s}\beta_j C_j/(1 + \beta_i C_i + \beta_j C_j) \quad (7)$$

where $\Gamma_{i,s}$ and $\Gamma_{j,s}$ represent the saturation coverages of i and j, respectively. The saturation coverages of the two anthraquinones considered here are experimentally indistinguishable, hence $\Gamma_{i,s}$ is equal to $\Gamma_{j,s}$ and is denoted simply as Γ_s. Equations 6 and 7 can provide estimates of the surface coverages of both 2,6-AQDS and 1,5-AQDS within binary monolayers as the composition of the deposition solution is systematically varied. This synthetic approach of controlling not only the total anthraquinone concentration, but also the ratio of the two derivatives, gives rise to modified surfaces with a wide range of compositions. Figure 9 shows the relationship between the values of the surface coverages predicted by eqs 6 and 7 and the values experimentally determined using high-speed chronoamperometry. This figure shows that the predicted and experimental values are highly correlated, that a near unity slope is observed, and that the experimental data are not biased. These observations strongly suggest that chronoamperometry can be used to determine not only the total surface coverage of anthraquinone but also the relative amounts of 2,6-AQDS and 1,5-AQDS within the superstructures.

In the following section, a strategy is presented that extends this kinetic approach to quantitation of species in solution. What is required is an expression for the concentration of species i in solution in terms of the saturation coverage, the coverages of the individual species, and the energy parameter. This objective can be attained by substituting into eq 7 the expression for $\beta_i C_i$ obtained from eq 6.[3]

$$C_i = \Gamma_i/(\Gamma_s - \Gamma_i - \Gamma_j)\beta_i \quad (8)$$

Therefore, by experimentally determining the partial coverages of 2,6-AQDS and 1,5-AQDS within binary

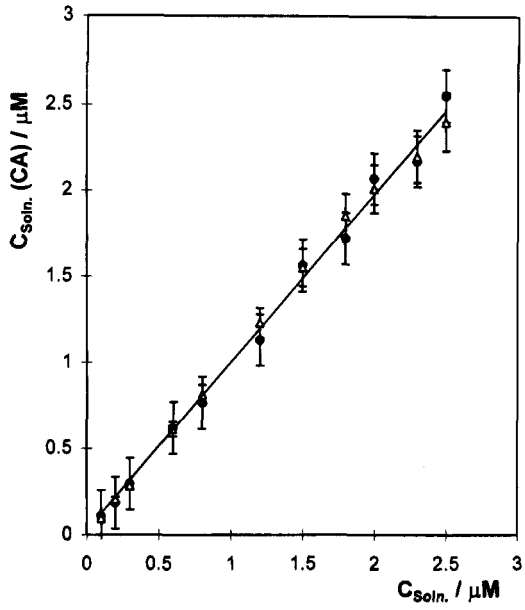

Figure 10. Relationship between the actual bulk concentrations of anthraquinones, C_{Soln}, and those predicted by eq 8 using high-speed chronoamperometric data, $C_{Soln}(CA)$. Data for 2,6-AQDS is denoted by Δ, while data for 1,5-AQDS is denoted by ●. The solid line indicates the behavior expected for a direct, unbiased correlation.

monolayers using high-speed chronoamperometry, it should in theory be possible to use eq 8 to determine their unknown concentrations in solution. It is important to note that conventional electrochemical approaches,[28] which depend on the individual components having different formal potentials for separation of their voltammetric responses, are completely unable to attain this objective.

Binary monolayers have been deposited from solutions in which the concentrations of 2,6-AQDS and 1,5-AQDS have been systematically varied. The high-speed chronoamperometric data obtained for these systems is similar to that shown in Figure 8 allowing the surface coverages of the two components within the monolayer to be determined on the basis of different kinetic rather than thermodynamic properties. These data have then been used in conjunction with eq 8 to estimate the bulk concentrations of the anthraquinones in solution. Figure 10 shows the relationship between the actual anthraquinone concentrations in solution and those estimated from the anthraquinone surface coverages using this new kinetic approach. Figure 10 shows that these data are highly correlated with a near unity slope, indicating that this kinetic approach can be successfully applied to determine the concentrations of surface active species in solution. Significantly, the linear regression line that models the experimental data shown in Figure 9 has an intercept that is close to zero, demonstrating that the experimental data are not biased. That this high-speed approach yields a strong unbiased correlation with the actual solution concentrations is especially significant when one considers the low concentrations of analyte involved. The solution concentrations are typically in the low micromolar range, emphasizing another advantage of this method, namely that the analyte of interest is preconcentrated onto the electrode surface.

Conclusions

Single component monolayers of 2,6-AQDS and 1,5-AQDS have been formed on mercury microelectrodes by equilibrium adsorption. The surface coverages and heterogeneous electron transfer rate constants have been determined using microsecond time scale chronoamperometry. The surface coverages obtained using cyclic voltammetry and chronoamperometry are experimentally indistinguishable. However, the heterogeneous electron transfer rate constant for 2,6-AQDS monolayers is more than 50 times larger than that obtained for 1,5-AQDS monolayers.

Binary monolayers containing both anthraquinones are formed by simultaneous coadsorption of the two molecules. The surface coverages of the two components cannot be determined using cyclic voltammetry because the formal potentials for the two molecules are experimentally indistinguishable. However, in a potential step experiment, the Faradaic current flow arising from oxidation of the two types of redox center can be separated in time because the two rates of interfacial electron transfer are different. This kinetic separation allows the surface coverages of the two anthraquinones to be determined even though their formal potentials are essentially identical.

By considering the competitive adsorption thermodynamics, this approach has been extended to allow the concentrations of species in bulk solution with coincident formal potentials, but different interfacial kinetics, to be determined amperometrically. This advance in electroanalysis has parallels with the technique of time-resolved fluorescence in photochemistry.[29] It is probable that in the future, new electroanalytical techniques will be developed that exploit the ability of microelectrodes to provide high-quality kinetic information at very short time scales. High speed electrochemical measurements are also advantageous in terms of discriminating against interfering background Faradaic processes. For example, because many of these interfering redox reactions occur on a milliseconds or even seconds time scale, they can be effectively eliminated by making the analytical measurement on a microsecond time scale.

Acknowledgment. The provision of high-speed electrochemical instrumentation by Professor Larry R. Faulkner of the University of Illinois at Urbana— Champaign, which made part of this work possible, is gratefully acknowledged.

LA940877+

(28) Kissinger, P. T. *Laboratory Techniques in Electroanalytical Chemistry*; Dekker: New York, 1984.

(29) Wolfbeis, O. S.; *Fluorescence Spectroscopy: New Methods and Applications*; Springer-Verlag: New York, 1993.